

5.3 Flow over an obstacle.

We now consider Froude number plane representation of a solution over topography in a channel of constant width. For this case it is helpful to rewrite the energy equation (5.2.13) in the normalized form

$$\frac{1}{2}F_1^{4/3} - \frac{1}{2}Q_r^{-2/3}F_2^{4/3} + F_1^{-2/3} = \frac{g'z_T^* - \Delta B}{(g'Q_1/w^*)^{2/3}} \quad (5.3.1)$$

One interpretation of the quantity on the right-hand side of (5.3.1) follows by imagining that the straight channel is connected to a wide, quiescent basin as described above. Use of (5.2.10) and (5.2.11) then leads to

$$\frac{g'z_T^* - \Delta B}{(g'Q_1/w^*)^{2/3}} = \frac{g'd_{1\infty}^*}{(g'Q_1/w^*)^{2/3}} = d_{1\infty}$$

The parameter $d_{1\infty}$ is the dimensionless upper layer thickness in the basin. It may also be regarded as a measure of the potential energy in the quiescent basin, smaller $d_{1\infty}$ being associated with higher interface values and therefore higher potential energy.

A family of solutions to (5.3.1) for $|Q_r| = 1$ and for various values of $d_{1\infty}$ are represented by the thick curves in Figure 5.3.1a. Internal energy is constant along each curve and, in the absence of hydraulic jumps or other dissipative features, a solution must follow a particular curve. Some of these curves intersect the critical flow diagonal, raising the possibility that corresponding solutions can be critically controlled. Others do not. Froude number diagrams for other values of Q_r have similar qualitative aspects (Armi, 1986) and we can therefore discuss most of the general features of the solutions using the one figure. Note that Q_r and Q_1 enter (5.3.1) as $2/3$ powers and therefore a solution curve valid for a combination (Q_r, Q_1) is also valid for $(-Q_r, Q_1)$, $(Q_r, -Q_1)$, or $(-Q_r, -Q_1)$. The direction of flow in a given layer for a particular solution is therefore arbitrary. Each location in Figure 5.3.1a formally yields different solutions corresponding to different directions of flow in the two layers. If one can establish a realizable solution that is valid for a given topography and upstream conditions, it is not always possible, however, to create another realizable solution by simply reversing the flow direction in one or both layers. Doing so can change the stability of the flow or its ability to form hydraulic jumps at certain locations. An obvious example is a unidirectional flow that is stable according to (5.2.2) but becomes unstable due to the increased interfacial shear that is created when the direction of flow in one of the layers is reversed. More subtle examples arise when the change in direction gives rise to the shock-forming instability (Figure 1.4.4) created at a critical section when a change in flow direction causes waves to converge at that section.

To find a solution for particular values of Q_2 , z_T^* , and w^* and for a given topography $h^*(y^*)$, we need to know how to move along the appropriate solid curve as h^*

varies. This link between the solution and to topography is provided by (5.2.14) and it is helpful to rewrite this equation as

$$Q_r^{2/3} F_1^{-2/3} + F_2^{-2/3} = q_2^{-2/3}, \quad (5.3.2)$$

where

$$q_2 = \frac{Q_2}{(z_T^* - h^*)^{3/2} g^{1/2} w^*}.$$

The thin contours drawn in Figure 5.3.1a are ones of constant q_2 . Since Q_2 , z_T^* , and w^* remain fixed for a particular solution, changes in q_2 are entirely due to changes in h^* . Increases in h^* lead to increases in q_2 and inspection of Fig. 5.3.1a shows that this generally corresponds to moving away from the origin.

Flow from a deep basin.

One important class of solutions describes flow originating from an infinitely deep upstream basin.¹ At least one of the layer depths must be infinite (and the corresponding velocity zero) in the basin and therefore the solution curve must begin along the horizontal ($F_2^2=0$) or vertical ($F_1^2=0$) axis in Figure 5.3.1a. Inspection of the figure shows that the only possibilities originate from the horizontal axis. These solutions have $F_2=0$ in the basin, meaning that the lower layer is infinitely deep and stagnant. The reverse situation, a stagnant upstream upper layer with a moving lower layer, is not possible. This asymmetry between the upper and lower layer is due to the fact that the obstacle contacts only the lower layer. Although the formal solutions allow the direction of flow within each layer to be arbitrary, let us assume that the lower layer flow is out of the deep basin. The upper layer flow may then be in either direction, unless otherwise noted. We will continue to refer to the latter as the upstream basin, even though the upper layer may flow into it.

Now suppose that the value of $d_{1\infty}$ is known to be 1.7, so that the solution must lie along the dark curve with that value. Keep in mind that $d_{1\infty}$ is not the actual upper layer depth in the deep basin, but rather the upper layer depth in a hypothetical reservoir that has infinite width and is therefore quiescent. This reservoir might be imagined to lie upstream of the deep basin. The flow state in the latter lies where the $d_{1\infty}=1.7$ curve intersects the F_1^2 axis and is clearly subcritical. An observer moving from the basin into the channel will see an increase in h and must therefore move upwards along the '1.7' curve to higher contour values of q_2 . If the sill is reached before the critical diagonal is encountered then the solution at points downstream is found by retracing the '1.7' curve back to the F_1^2 axis. In this way a completely subcritical solution is obtained. The value

¹ Since the deep basin has finite width, the parameter $d_{1\infty}$ should not be interpreted as the upper layer depth; the upper layer may be moving. However, one could imagine the deep basin broadening into an infinitely wide basin as some point even farther upstream, and here $d_{1\infty}$ would indeed represent the upper layer depth.

of F_1^2 is minimal at the sill, meaning that the interface elevation is also minimal (see 5.2.12a). Figure 5.3.1b shows this situation schematically, with the ‘1.7’ solution curve traced over a circuit aba and the corresponding subcritical solution (shown in the inset) experiencing an interfacial dip over the obstacle.

If the sill height is increased to the point where the sill is encountered at the crossing with the critical diagonal, then a transition to supercritical flow is possible. Note that the dark and light contours make grazing contact with each other along the critical diagonal, implying that the solution may be followed beyond the sill either by continuing along the ‘1.7’ curve into the supercritical region or by retracing back into the subcritical region. This same dilemma arises in the treatment of single-layer flows and it can be shown by similar arguments (see Section 1.4 or Exercise 4 of the previous section) that the correct option is to continue into supercritical space. The circuit is something like $abcd$ in Figure 5.3.1b and the interface profile resembles the free surface profile for a hydraulically controlled, single-layer flow.

If the sill height is increased beyond its critical value for the ‘1.7’ energy curve then the solution cannot lie along that curve. In this case an upstream disturbance is generated that adjusts Q_1 , Q_2 , and/or $d_{1\infty}^*$ to new values needed to maintain critical flow at the sill. This process is described in more detail below.

Given the similarity with the single-layer case, one might expect a hydraulic jump to arise in the supercritical part of the flow. The problem of shock joining in two layers is more difficult than for the single-layer case due to several factors. First, momentum transfers between the two layers can occur as the result of pressure forces on the steeply sloping interface within a jump. These forces exist in the region where nonhydrostatic effects are expected to be greatest, making calculation of the pressure force problematic. The difficulty is avoided in single layers due to the fact that the pressure is essentially zero at the free surface. Second, entrainment of one layer into the other or creation of masses of intermediate density can occur as the result of mixing. These transformations complicate the mass balances. In some cases interfacial instability and mixing occur broadly and cause the transition from supercritical to subcritical flow to occur without any roller or other abrupt feature. An example of this limiting case is shown in the top frame of Figure 1.6.5.

One situation that allows simplification occurs when the two fluids are immiscible, so that Q_1 and Q_2 are conserved across the jump. If the jump occurs over a small interval in y^* , so that h^* is the same on either side, then the conjugate states must occur along the same constant- q_2 curve. As an example, suppose that a hydraulic jump occurs at point d in Figure 5.3.1b. The jump must return the supercritical flow to a subcritical state and must do so along the thin curve passing through d . It must therefore connect with another constant energy curve, perhaps at point e . Determination of the correct energy curve is quite difficult, however. The jump should cause an overall loss of total energy and it is not obvious what this means for ΔB , the difference between the upper and lower layer

Bernoulli functions². There have been a number of attempts to come to grips with these problems and the reader is referred to Jiang and Smith (2001a,b) and references contained therein for more information.

Maximal Flow

Up to this point, the presence of an upper layer has introduced nothing qualitatively new; the lower layer acts like a single layer. However, novel effects come into play if the interface level in the hypothetical reservoir is raised ($d_{1\infty}$ is decreased). This change could be effected by demanding that Q_1 and Q_2 remain fixed, that the sill flow remain critical, and that the sill height (and therefore q_2) be increased. The new sill flow is found by following the critical diagonal from point c in Figure 5.3.1b down and to the right until the thin curve with the new value of q_2 is encountered. The solution now lies along the (thick) energy curve that intersects this point, and it can be seen that the corresponding $d_{1\infty}$ is lower than before. The new energy curve intersects the F_1^2 axis at larger values of F_1^2 than before and thus the composite Froude number G^2 of the upstream flow is greater. The upper layer in the basin now has a higher velocity and smaller thicknesses. If the sill height is increased further, the upper layer Froude number in the basin continues to increase. Eventually the value $d_{1\infty}=1.5$ is eventually reached and it can be seen that the corresponding energy curve has an intersection with the F_1^2 -axis at $F_1^2=1$. The flow in the basin is now critical. Since the basin is infinitely deep, the lower layer remains at rest and the upper layer moves at speed $v_1^*=(g'd_1^*)^{1/2}$. The value of G^2 is unity both in the basin and at the sill and the flow therefore has two control sections. In the case where the both layers flow out of the basin the upstream control is called an *approach control*. In an exchange flow, where the direction of the upper layer is reversed, the basin control is called an *exit control*. The flow is subcritical between the two controls and is supercritical downstream of the sill, perhaps with a hydraulic jump. The situation is represented by the solution *ghi* in the Figure 5.3.1b inset. In the idealized geometry of this example, the upper layer flows at the critical speed far into the upstream basin. A uniform critical flow of this type is typically vulnerable to frictional and dispersive effects. A more stable version of the solution can be set up if variations in the upstream width are allowed, as discussed below.

The solution with both a sill control and an approach control has been obtained by allowing the value of $d_{1\infty} = \frac{d_{1\infty}^*}{(g'Q_1/w^*)^{2/3}}$ to decrease until the upper layer in the basin becomes critical. Since $d_{1\infty}^*$ is a measure of the internal energy of the flow the decrease in $d_{1\infty}$ can be accomplished by holding the energy constant and increasing $|Q_1|$. The threshold state $d_{1\infty}=1.5$ may therefore be regarded as having the maximum possible upper layer transport for the given available internal energy. As Figure 5.3.1a shows, this value cannot be exceeded by any solution that connects smoothly to a deep upstream

² The simplest approach [suggested by Armi (1986)] is to assume that the energy loss in the jump is negligible, so that the conjugate states lie on the same energy curve.

basin. There are solutions with larger $|Q_1|$ (i.e., the ones with $d_{1\infty} > 1.5$) but none intersect the lower axis.

For flows with only a sill control ($d_{1\infty} > 1.5$) the behavior of the lower layer is similar in most respects to a single layer. The upper layer is relatively unimportant. For example, it can be shown that the layer Froude numbers at the sill fall in the ranges $0.8 < F_2^2 < 1$ and $F_1^2 < 0.2$. Thus the lower layer Froude number is close to the critical value (=1) for a single layer whereas the upper layer Froude number is well into the subcritical range of a single layer. The wave arrested at the sill is dynamically similar to a wave propagating in an environment in which the upper layer is inactive. In contrast, the solution for $d_{1\infty} < 1.5$ involves engagement of both layers. The approach (or exit) control takes place where the lower layer is inactive and the sill control takes place where the upper layer is relatively inactive.

For exchange flows it is common to refer to the solution with both a sill control and an approach control as being *maximal*. It has the largest $|Q_1|$, and therefore the largest exchange transport $|Q_1 - Q_2|$, of all the solutions that can smoothly be connected to a deep basin. The maximization assumes that Q_r remains fixed. Solutions with just sill controls ($d_{1\infty} > 1.5$) are called *submaximal*. Note that the extremities of the solution curves with $d_{1\infty} < 1.5$ extend to $F_1^2 \rightarrow \infty$ in one direction and $F_2^2 \rightarrow \infty$ in the other, and therefore cannot be smoothly be linked to infinitely deep upstream basins.

Basins with Finite Depth

If the upstream basin has finite depth, identification of the submaximal and limiting maximal solutions is just slightly more difficult. The previously considered constant-energy curves are still in play, but the possible upstream states now lie at finite F_2 and not along the abscissa of the Froude number plane. In order to fix the parameter $d_{1\infty}$ we continue to imagine that the actual upstream state is connected to a hypothetical basin with infinite width and having a known interface elevation. The parameter $d_{1\infty}$ is the upper layer thickness corresponding to this upstream elevation and its value determines the energy curve that defines the solution. Suppose that this value is 1.7, so that the solution lies along the left-most energy curve in Figure 5.2c. Then we can construct a variety of solutions with different fluxes as before. If it is known in advance that the solution is controlled at the sill section, then the flux magnitude $|Q_1|$ (or $|Q_2|$) is determined from the q_2 value that exists where the $d_{1\infty} = 1.7$ curve intersects the critical diagonal.

One may then consider the family of controlled but submaximal solutions for successively smaller values of $d_{1\infty}$. A limiting maximal solution will eventually be obtained, this time with a value < 1.5 . An example is shown by the curve segment *klmn* in Figure 5.3.1b. The upstream flow in the uniform, finite-depth section of channel (*k* in the figure) is an approach (or 'exit') control. Once the bottom begins to shoal, the flow

becomes subcritical (l). It then passes through a sill control (m) and becomes supercritical (n). A profile of the solution is sketched in the inset.

The limiting solution curve that determines the maximal solution for a given finite upstream depth is not easy to locate. However the curve and its $d_{1\infty}$ value can be calculated and shown to depend on the ratio of the depth D_s over the sill to the upstream depth z_T^* . By applying the definition of q_2 at the upper left intersection of the energy curve with the critical diagonal (i.e. at the sill control) it follows that

$$|Q_2| = q_2(D_s / z_T^*) g'^{1/2} w^* D_s^{3/2}. \quad (5.3.3)$$

The function $q_2(D_s/z_T^*)$ is simply q_2 at the upper left intersection point and the calculation of its dependence on D_s/z_T^* is described in Exercise 5. For the case of an infinitely deep upstream basin $D_s / z_T^* \rightarrow 0$ q_2 is given by .208, whereas $q_2=0.25$ for the point labeled o . As D_s / z_T^* increases so does the associated q_2 and thus the maximal flux for fixed D_s and g' increases as the upstream depth decreases. That these flows are choked to a lesser extent is due to the fact that the sill height h_m^* is a smaller percentage of the upstream depth z_T^* .

Although (5.3.4) bears similarity to the single-layer weir formula (1.4.12), it is more constrained. It is no longer necessary to have knowledge of an upstream interface elevation or the like; the only dynamic variable that needs to be measured is the reduced gravity g' . The insensitivity of the flux to upstream conditions is consistent with the existence of the 'exit' or 'approach' control, which blocks mechanical information from reaching the sill. The relevance of g' is consistent with the fact that density is advected by the flow and information about the density difference $\Delta\rho$ can pass right through the control section. The value of g' has been regarded fixed throughout this discussion, but one would wish to eventually relax this constraint by allowing $\Delta\rho$ to vary, say in response to changes in forcing and/or mixing in the upstream basin. This topic will be pursued in Section 5.3.

If the sill elevation h_m^* is decreased to zero, so that $D_s / z_T^* = 1$, the upstream and sill controls merge. The coalescence point *lies* at o (5.3.1b) where the critical diagonal makes grazing contact with the curve $d_{1\infty}=1.25$. It can be shown (see Exercise 2) that both c_+ and c_- are zero in this solution, which will emerge as an important type of flow through a contraction. The corresponding lower layer transport is given by

$$|Q_2| = (1 + |Q_r|^{1/2})^{-2} g'^{1/2} w^* D_s^{3/2} \quad (5.3.4)$$

(see Exercise 6), where D_s is now just the depth in the uniform channel. Larger values of $|Q_2|$ correspond to (supercritical) solution curves lying entirely above the critical diagonal. These solutions do not connect directly to any geophysically relevant reservoir state, nor is it possible to connect the solutions to subcritical flow by hydraulic jumps

along curves of constant q_2 . Therefore (5.3.4) gives an upper bound on $|Q_2|$ for relevant flow (i.e. flows that become subcritical somewhere upstream).

Other Constraints

In most cases of geophysical or engineering interest, geometrical variables like w^* , h_m^* , and z_T^* are known in advance and $d_{1\infty}^*$ can be estimated from hydrographic data. In addition, a relation between Q_1 and Q_2 can often be stipulated, such as when the strait connects with a closed basin with known evaporation E and precipitation P . (The flow rates are then constrained by $Q_1 - Q_2 = \iint_{A_s} (E - P)dA$, where A_s is the surface area of the basin.) These constraints are still insufficient to determine the parameters $d_{1\infty}$, q_2 , and Q_r required to fix the solution and the individual values of Q_1 and Q_2 . To do so, one must assume that the solution is critical at the sill, and perhaps in the approach, and use these conditions to close the problem.

As an example, consider the case where the upstream basin is infinitely deep and it is suspected that an approach (or exit) control *and* a sill control occur ($d_{1\infty}=1.5$). For exchange flow, this would mean that the exchange transport is maximal. Further assume that the downstream basin is closed and has $\iint_{A_s} (E - P)dA = 0$, so that $Q_r = -1$. We have already shown that $Q_2 = -Q_1 = .208 g^{1/2} w^* D_s^{3/2}$ under these conditions. If $|Q_r| \neq 1$, then a more general version of the last relation (Exercise 3) can be used. If it is known that only a sill control exists, then the flux is just one of a continuum of values, each with its own $d_{1\infty}$. It now becomes necessary to measure the upstream interface level in order to close the problem.

Laboratory and numerical experiments on two-layer sill flows.

To further digest the properties of the flows under consideration it can be helpful to consider how they are established. We discuss two revealing experiments, the first dealing with unidirectional flows and the second with exchange flows. The first was originally performed by Long (1954, 1970) who towed an obstacle through a two-fluid system initially in a state of rest. Extensions have been carried out by Houghton and Isaacson (1970), Baines (1984, 1987), and others. The typical setting for numerical computation of the flow has two layers moving from left to right at equal speeds ($Q_r=1$) in a uniform channel ($h^*=0$). Consider the case where this initial flow is subcritical and where $F_1^2 \ll F_2^2$, so that the upper layer is relatively deep and inactive. For example, we could assume that the initial state lies at point *b* in Figure 5.3.1b. At $t^*=0$ an obstacle of height h_m^* is placed in the path of the flow. The adjustment for moderate h_m^*/z_T^* is similar to that for a single-layer flow. If $h_m^*/z_T^* \ll 1$, the flow remains subcritical and there is no upstream influence. As h_m^*/z_T^* is increased, a critical value will be reached above which upstream influence occurs. The critical value is that required to move the solution from point *b* to point *c* in Figure 5.3.1b. The steady solution that develops over

the obstacle will resemble solution *bcd*. A slight increase in h_m^*/z_T^* past the critical value will result in the excitation of an upstream disturbance that will permanently alter the upstream flow by deepening the lower layer and decreasing the lower layer transport. Further incremental increases in h_m^*/z_T^* will have a similar effect. As long as the upper layer remains relatively inactive during this process, the linear waves speed ($c_* \equiv v_2^* - (g'd_2^*)^{1/2} < 0$) of the upstream flow increases in magnitude. As the obstacle height increases, it is possible for the lower layer to become completely blocked as a result of this process and further increases in h_m^*/z_T^* will cause the obstacle to protrude into the upper layer. In this case, additional changes to the upstream are prevented.³ Up to this point the evolution is similar to that found in the single-layer version of Long's experiment (Section 1.6).

If the lower layer remains unblocked, increases in h_m^*/z_T^* eventually lead to effects that are special to two-layer systems. To understand these changes, it must first be recognized that growth of the obstacle does not alter the total volume transport $Q_1 + Q_2$. Thus, the decrease in Q_2 is compensated by an increase in Q_1 . In addition, the upstream thickening of the lower layer results in a thinning of the upper layer. Both effects tend to bring the initially inactive upper layer into play upstream of the obstacle, and the main effects is to reduce the magnitude of c_* . As h_m^*/z_T^* increases, c_* reaches a maximum negative value then moves towards positive values. At some h_m^*/z_T^* this trend causes the upstream flow to become critical $c_* = 0$. The flow over the obstacle now resembles the solution *klmn* of Figure 5.3.1b, with approach and sill controls. (The reader is cautioned, however, that Q_T may no longer be unity and therefore Figure 5.3.1b may no longer apply.) *Numerical simulations have shown that further increases in h_m^*/z_T^* causes flow over the obstacle to revert to a supercritical, symmetrical state, while the approach control is maintained.* The flow near the obstacle now resembles solution *kjk*. Beyond this point, increases in h_m^*/z_T^* lead to no further upstream influence.

There are some variations to this chain of events and many subtleties that have not been mentioned. The reader is referred to Baines (1995, Chapter 3) for more details. A fundamental point to keep in mind is that formation of the approach control, the central departure from single-layer hydraulics, occurs because $-c_*$ has a maximum value in the upstream flow at an intermediate interface level.

It is not obvious that the flow with both approach and sill controls (and presumably subcritical flow in between) transits to a state with only an approach control and supercritical flow over the obstacle. Why not have an approach control with subcritical flow over the sill? Perhaps such a state would be unstable; disturbances created at the sill would propagate to the upstream edge of the obstacle but would be arrested there. If this is the case, then doesn't the same argument apply to the maximal solution?? Also, it appears from the experiment that the solution with approach and sill controls is one that occurs for a particular sill height and not a range of sill heights. On the other hand, flows with just a sill control or just an approach control occur over a range of

³ Additional increases in the obstacle height will only impede the upper layer flow if frictional or non-hydrostatic effects come into play.

sill heights. This makes it hard to see how the ‘maximal’ solution could actually arise in nature.

An experiment showing maximal and submaximal exchange flows in a laboratory channel was performed by Zhu and Lawrence (2000). As shown in Figures 5.3.2(a,b), the channel contains an isolated obstacle and opens abruptly at either end into wide reservoirs. The right and left reservoirs initially are filled to the top with fluids of slightly different densities, the left reservoir containing the denser fluid. A barrier that sits atop a sill separates the two fluids. The barrier is removed and the two fluids are allowed to displace each other. After an initial period of transient activity, the flow within the channel settles into a nearly steady state. The layer velocities in the left reservoir are relatively weak and the upper layer depth therefore approximates $d_{1\infty}^*$. Initially, this depth is relatively small (Figure 5.3.2c), but it gradually increases as lower layer fluid is drained out of the reservoir. An exit control occurs near the left end of the channel (point k) and the flow immediately to the right is subcritical. To the left there is a brief span of supercritical flow that is linked to the reservoir by something like a hydraulic jump. The flow near the jump is horizontally two dimensional due to the abrupt widening of the geometry. At the sill the subcritical flow passes through a second control and becomes supercritical. A hydraulic jump occurs on the right slope of the obstacle and the flow thereafter is subcritical. From the left end of the channel to the hydraulic jump the interface resembles the solution $klmn$ of Figure 5.3.1b. The transition from the left end of the channel into the left reservoir cannot be traced in this figure but is discussed below. While in this configuration, $|Q_1 - Q_2|$ remains fixed at its maximal value, the determination of which is described in Exercise 4.

As the left reservoir loses lower-layer fluid, the interface there falls and the hydraulic jump moves closer to the entrance (point k) of the channel. At the same time, conditions in the channel between the exit control and the sill control remain steady; the supercritical end states insulate that part of the flow from the two reservoirs. However, the interface in the left reservoir eventually becomes low enough that the hydraulic jump reaches the position of the exit control. The exit control becomes ‘flooded’, the flow there becomes subcritical, and the exchange becomes submaximal and dependent on the upstream interface elevation. This elevation continues to decrease and with it the exchange flux.

Exercises

- 1) For arbitrary Q_r , which constant energy curve makes grazing contact with the critical diagonal in Figure 5.3.1a?
- 2) For the solution designated by the point o in Figure 5.3.1b, prove that under conditions of pure exchange flow, $c_+^* = c_-^* = 0$.
- 3) Consider the case of flow over an obstacle and originating from an infinitely deep basin. If the flow has an approach control and a sill control, show that $d_{1\infty}^* = 1.5$ regardless

of the value of Q_r . Further show that the transport in the lower layer is given the generalized weir formula:

$$Q_2 = [Q_r^{2/3} F_{1c}^{-2/3} + (1 - F_{1c}^2)^{-1/3}]^{-3/2} g^{1/2} w^* D_s^{3/2},$$

where F_{1c} is determined from

$$F_{1c}^{4/3} - Q_r^{-2/3} (1 - F_{1c}^2)^{2/3} + 2F_{1c}^{-2/3} = 3.$$

4) In the experiment of Zhu and Lawrence (2000), described in part *c*, a maximal exchange flow was observed. The values of w^* , g' , z_T^* , and h_m^* are set by the geometry and by the initial conditions and it is also known, due to the closed geometry of the channel and reservoir system, that $Q_r = -1$. To predict the maximal value of Q_2 :

(a) Show that

$$F_{1e}^{4/3} - (1 - F_{1e}^2)^{2/3} + 2F_{1e}^{-2/3} = F_{1s}^{4/3} - (1 - F_{1s}^2)^{2/3} + 2F_{1s}^{-2/3},$$

where the subscripts *e* and *s* correspond to exit and sill. (Hint: use energy conservation between the exit and sill along with the critical condition at both locations.)

(b) Further show using volume flow rate continuity that

$$\begin{aligned} Q_2 &= g'^{1/2} w^* (z_T^* - h_m^*)^{3/2} [F_{1s}^{-2/3} + (1 - F_{1s}^2)^{-1/3}]^{-3/2} \\ &= g'^{1/2} w^* (z_T^*)^{3/2} [F_{1e}^{-2/3} + (1 - F_{1e}^2)^{-1/3}]^{-3/2}. \end{aligned}$$

This gives three equations for the unknowns F_{1e}^2 , F_{1s}^2 , and Q_2 in terms of the known w^* , z_T^* , etc.

5) *Calculation of the coefficient $q_2(D_s / z_T^*)$ in equation 5.3.3.* Consider a solution for flow in a channel with constant width and with $|Q_r| = 1$. The flow has two control points corresponding, say, to points *k* and *m* in Figure 5.3.1b. Show that the values of the lower layer Froude numbers at *k* and *m* can be computed from the relations:

$$\frac{Q_r^{2/3} F_{1m}^{-2/3} + (1 - F_{1m}^2)^{-1/3}}{Q_r^{2/3} F_{1k}^{-2/3} + (1 - F_{1k}^2)^{-1/3}} = \frac{D_s}{z_T^*}$$

and

$$\frac{1}{2} F_{1m}^{4/3} - \frac{1}{2} Q_r^{-2/3} (1 - F_{1m}^2)^{2/3} + F_{1m}^{-2/3} = \frac{1}{2} F_{1k}^{4/3} - \frac{1}{2} Q_r^{-2/3} (1 - F_{1k}^2)^{2/3} + F_{1k}^{-2/3}.$$

Here z_T^* is the total depth upstream of the obstacle (where $h^*=0$). Once F_{1m} has been calculated from these relations, F_{2m} follows from the critical condition $G^2=1$. Then q_2 follows from (5.3.2).

Figure Captions

Figure 5.3.1 (a) The Froude number plane showing solution curves for flow over a variable bottom in a channel width constant width and the $|Q_r|=1$. Contours of constant internal energy $d_{1\infty}$ are represented by thick lines. Continuous solutions must lie along these contours. The thin contours represent constant q_2 . For a fixed layer flux Q_2 , larger values of the topographic height h^* correspond to smaller q_2 .

Figure 5.3.1 (b) A portion of the Froude number plane with examples of various solutions sketched in the insets.

Figure 5.3.2 The experimental setup used by Zhu and Lawrence (2000) to simulate a lock exchange.

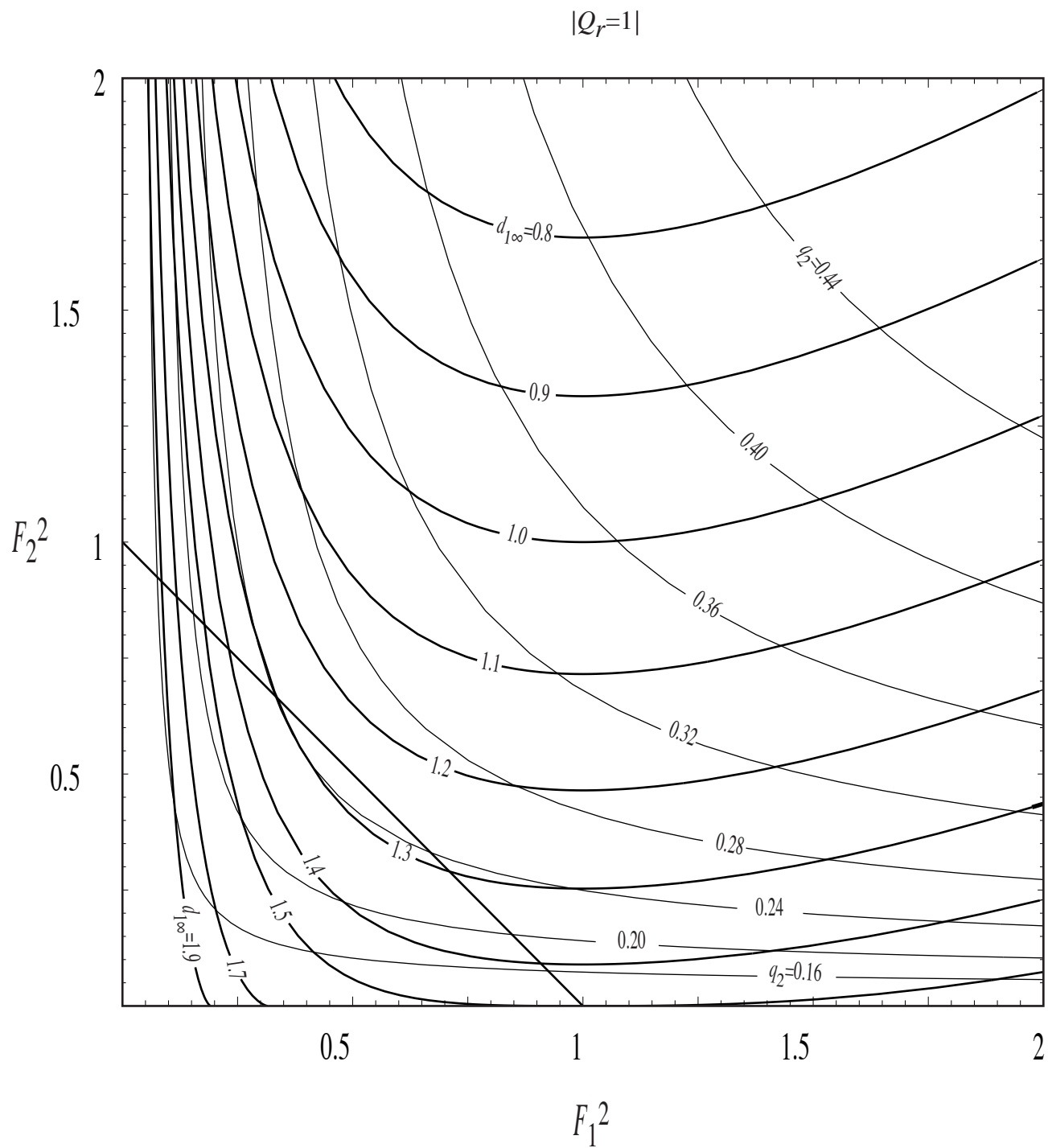


Figure 5.3.1a

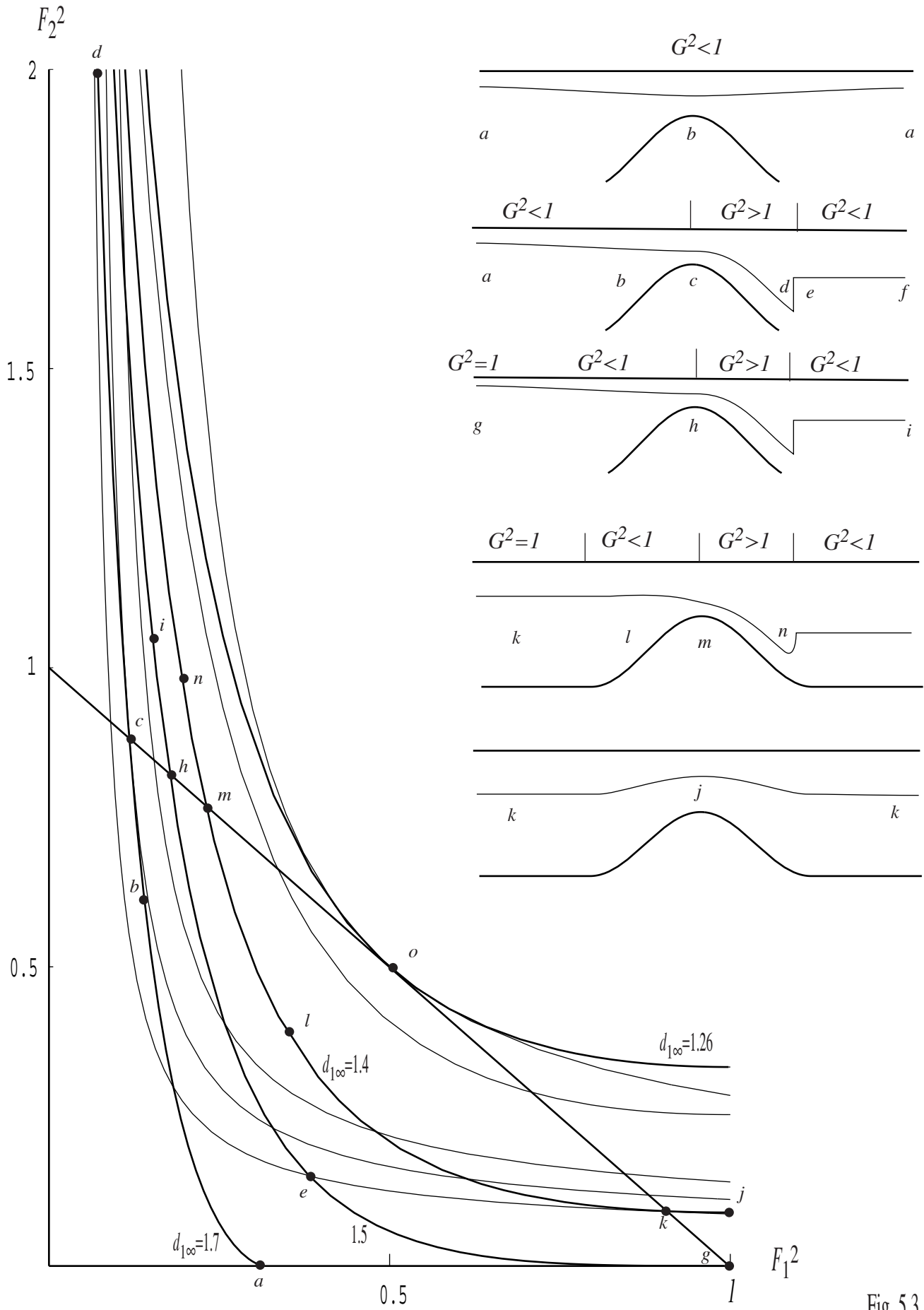


Fig. 5.3.1b

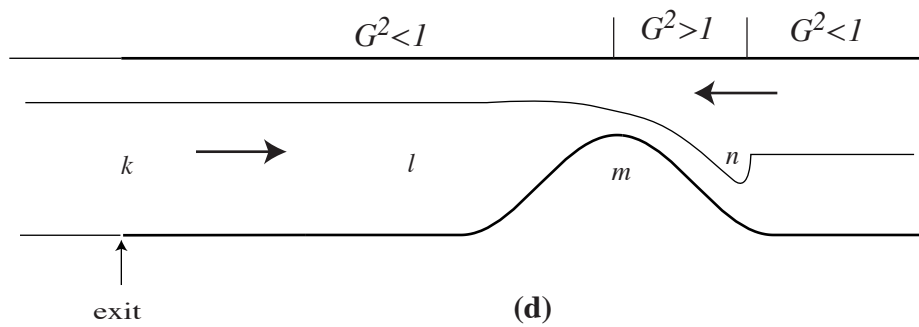
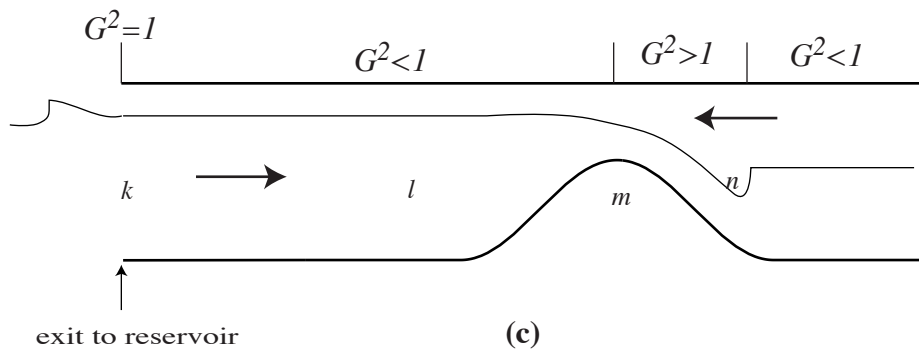
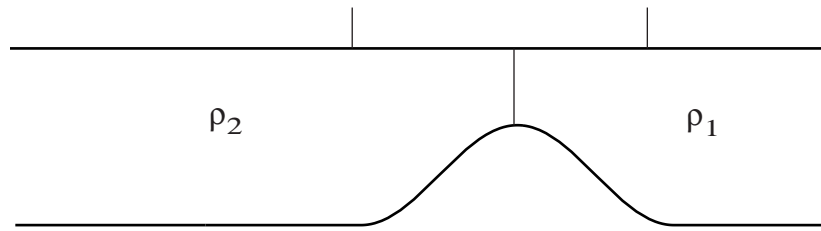
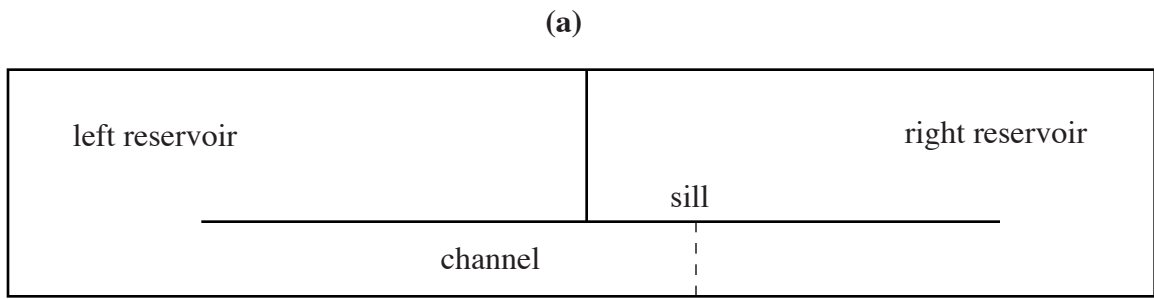


Fig. 5.3.2